ACTIVE POWER CONTROL IN PV SYSTEMS BASED ON A QUADRATIC CURVE FITTING ALGORITHM FOR THE MPP ESTIMATION

Efstratios BATZELIS[(1)] Sotirios NANOU[(1)] Stavros PAPATHANASSIOU[(1)]

[(1)] NTUA, Electric Power Division, 9 Iroon Politechniou str., 15780, Athens, Greece

e-mail: batzelis@mail.ntua.gr, sotnanou@gmail.com, st@power.ece.ntua.gr

ABSTRACT: In this paper, an active power control strategy is presented in order for a PV plant to operate at a specified suboptimal output power setpoint and maintain power reserves, expressed as a fraction of the maximum available power. Given that the latter is not known a priori, a quadratic curve fitting algorithm is applied to recent past measurements in order to estimate the *P-V* curve and calculate the operating voltage to achieve the desired power reserve levels. The proposed method offers sufficient accuracy, increased robustness and computational efficiency, combined with excellent dynamic response at irradiance variations and reserve command changes. The effectiveness of the control strategy and the *P-V* curve estimation method is validated by simulations in MATLAB/Simulink.
Keywords: Curve Fitting, Linear Least Squares, MPP Estimation, Photovoltaic System, Quadratic, Reserves.

1 INTRODUCTION

The increasing penetration of photovoltaic (PV) generation worldwide raises system integration issues for the operators of the grid. To allow large-scale penetration of PV and other intermittent renewable energy sources (RES) technologies, there is a demand for the stations to provide ancillary services to the grid, such as frequency response. Moreover, in isolated electrical networks with high PV capacity, such as small islands, the thermal stations are often forced to operate at minimum output, imposing the need for active regulation of PV plant output power. These services may be offered by a PV system if it is capable of maintaining active power reserves and controlling its output power, in response to commands issued by the grid operator.

The standard solution to implement power regulation capabilities in a PV plant is to employ energy storage, such as batteries or even ultra capacitors [1]-[2]. However, this approach entails increased capital and maintenance cost, as well as additional system complexity [3]. An alternative approach is to operate the PV plant at a suboptimal operating point, rather than at the maximum power point (MPP), thus offering a power reserve to provide frequency response with up/down-regulation of its output. A thorough literature review of active power control schemes is presented in [3]. In [4], a strategy of suboptimal operation is presented, employing a PV array voltage level specified as a percentage of the open circuit voltage, but a quantification of the curtailed output power is not provided to support reserve commands. Similar frequency control schemes may be found in [5]-[6], based on droop type controllers, and in [7], presenting a one-stage control strategy. These methods do not treat regulation of PV power at a given setpoint, maintaining specific power reserves.

In [8], such a two-stage control scheme is studied, introducing a hybrid linear/quadratic estimation method for the maximum available power P_{max}. However, the determination of P_{max} in [8] lacks in practical implementability mainly due to the need for MPP voltage knowledge and the susceptibility to noise in measurements. In this paper, a curve fitting technique is proposed for estimation of the *P-V* curve and the MPP, which is integrated into a power control scheme similar to [8] and [14]. The proposed estimation method combines low computational cost, increased robustness and relatively simple implementation.

The power control scheme of the DC/DC converter is presented in Section 2, while the quadratic curve fitting estimator of the *P-V* curve is analyzed in Section 3. The validity of the proposed method is verified by simulations in Section 4, and conclusions are summarized in Section 5.

2 POWER CONTROL SCHEME

A boost DC/DC converter is used to regulate the output voltage of the PV generator to the appropriate levels in order to maintain the specified power reserves (Figure 1). Assuming that the dc link voltage is kept constant by the control of the inverter, adjustment of the duty cycle *D* of the PWM leads to regulation of the PV generator's operating point.

D is determined by a PI controller which utilizes the mean operating voltage V_m over a control period and the reference voltage V_{ref} calculated by the *Quadratic Curve Fitting Estimator*. The latter employs a linear least squares curve fitting algorithm on a set of recent past measurements (V_m, I_m), in order to fit a quadratic polynomial to the *P-V* curve of the PV generator. This is subsequently used to estimate the maximum available power P_{max}, and thus the reference power P_{ref} after accounting for the desired reserve levels *r*. Thereafter, the polynomial equation is utilized to determine the reference voltage V_{ref} from the reference power P_{ref}. The method is described in detail in the following section.

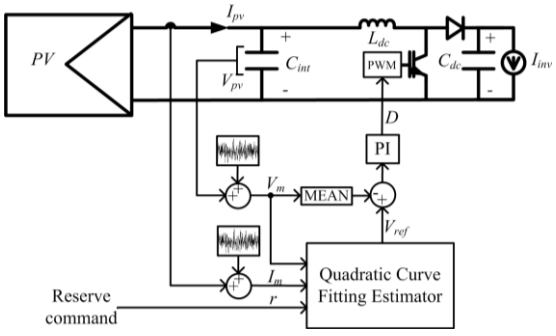

Figure 1: Topology and control scheme of the DC/DC converter.

Furthermore, the proposed control scheme is inherently designed for noisy environment, which is simulated by assuming a noise signal superposed on measurements (additive white gaussian noise - AWGN) (Figure 1). Thus, the operating voltage utilized by the PI controller is the mean of the voltage values over the control period, instead of the last recorded value. Since the duty cycle D remains constant during a control period, averaging the V_m samples removes switching ripple and noise (zero noise mean value). In addition, the curve fitting technique over a large set of past measurements is inherently more robust and reliable in presence of noise, compared to other approaches which utilize only a few previous samples [8], [10]-[11].

2 QUADRATIC CURVE FITTING ESTIMATOR

The main prerequisite for the implementation of the control scheme of Figure 1 is a reliable estimator of the available maximum power P_{max}, when operating at a suboptimal point, possibly far from the MPP. In [8], an empirical estimation method is considered, which utilizes two subsequent measurements (current and previous operating points) to approximate the *P-V* curve in a combined linear-quadratic way, and then to determine P_{max} using the known MPP voltage (which is considered to be an input). However, the dependence of this approach on only two measurements makes it susceptible to measurement noise and errors, while the knowledge of the MPP voltage is a limitation. In [7], a simple quadratic estimation based on [10] is considered, which makes use of three operating points to estimate P_{max} in a frequency regulation strategy. Yet, the proposed control scheme is intended for near-MPP operation. Another interesting relevant approach may be found in [11], in which a high-order polynomial approximation for the *P-V* is employed. Still this method is implemented for MPP operation and presents increased computational cost, since numerical evaluation of the polynomial equation is involved.

In this paper a curve fitting algorithm is introduced, in which the simple quadratic function is fitted to a set of previous measurements to approximate the *P-V* characteristic, and therefore P_{max}. Assuming that the power-voltage relation may be expressed in the simple quadratic form, $P = AV^2 + BV + C$, the proposed method fits this equation to a certain number of past measurements, included in a measurement window, in order to determine the parameters *A*, *B* and *C*. Thereafter, the MPP is calculated as the maximum of the estimated *P-V* relation in terms of the three parameters:

$$\hat{P}_{max} = C - \frac{B^2}{4A} \qquad \hat{V}_{max} = -\frac{B}{2A} \tag{1}$$

Given $\hat{P}_{max}$, the desired power output P_{ref} is simply:

$$P_{ref} = (1-r)\hat{P}_{max} \tag{2}$$

and the corresponding V_{ref} is then calculated by:

$$V_{ref} = \frac{-B - \sqrt{B^2 - 4A\left(C - P_{ref}\right)}}{2A} \tag{3}$$

The block diagram of the overall procedure is depicted in Figure 2. The curve fitting algorithm is applied to a window of *k* previous measurements ($V_{1,2,\ldots,k}$, $I_{1,2,\ldots,k}$), while the estimated coefficients of the quadratic polynomial *A*, *B* and *C* are low-pass filtered to suppress undesired high-frequency ripple.

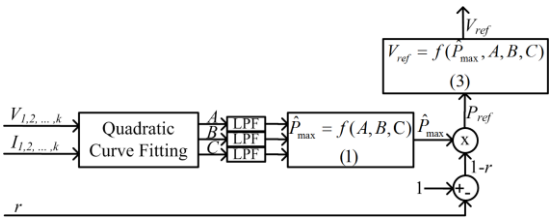

Figure 2: Block diagram of the Quadratic Curve Fitting Estimator**.**

In Figure 3, the curve fitting method is demonstrated graphically. Given the measurement window of past measurements (V_i, P_i) (blue dots for noiseless environment – red dots for a slightly noisy environment), the least squares method minimizes the sum of squared ordinal deviation between estimated and measured values, by zeroing the partial derivatives with respect to each parameter *A*, *B* and *C* [12]. In the case of linear combination of the parameters, the theorem of linear least squares curve fitting states that the estimated values are calculated by [11]:

$$\begin{bmatrix} V_1^2 & V_2^2 & \ldots & V_k^2 \\ V_1 & V_2 & \ldots & V_k \\ 1 & 1 & \ldots & 1 \end{bmatrix} \begin{bmatrix} V_1^2 & V & 1 \\ V_2^2 & V_2 & 1 \\ \vdots & \vdots & \vdots \\ V_k^2 & V_k & 1 \end{bmatrix} \begin{bmatrix} A \\ B \\ C \end{bmatrix} = \begin{bmatrix} V_1^2 & V_2^2 & \ldots & V_k^2 \\ V_1 & V_2 & \ldots & V_k \\ 1 & 1 & \ldots & 1 \end{bmatrix} \begin{bmatrix} P_1 \\ P_2 \\ \vdots \\ P_k \end{bmatrix} \tag{4}$$

Multiplication of the matrices leads to the simpler equation (5), in which the sums of measurements $S_{xy} = \sum_{i=1}^{k} V_i^x P_i^y$ are used instead of their individual values:

$$\begin{bmatrix} S_{40} & S_{30} & S_{20} \\ S_{30} & S_{20} & S_{10} \\ S_{20} & S_{10} & S_{00} \end{bmatrix} \begin{bmatrix} A \\ B \\ C \end{bmatrix} = \begin{bmatrix} S_{21} \\ S_{11} \\ S_{01} \end{bmatrix} \tag{5}$$

This is a simple system of three linear equations which leads to explicit closed-form expressions for parameters *A*, *B* and *C* in terms of the sums S_{xy}. However, the values of S_{xy} may differ by several orders of magnitude, possibly leading to numerical inaccuracies if not properly manipulated. Therefore, equation (5) may be rewritten using normalized versions of the parameters involved:

$$\begin{bmatrix} s_{40} & s_{30} & s_{20} \\ s_{30} & s_{20} & s_{10} \\ s_{20} & s_{10} & s_{00} \end{bmatrix} \begin{bmatrix} a \\ b \\ c \end{bmatrix} = \begin{bmatrix} s_{21} \\ s_{11} \\ s_{01} \end{bmatrix} \tag{6}$$

where $s_{xy} = \sum_{i=1}^{k} \left(\frac{V_i}{V_n}\right)^x \left(\frac{P_i}{P_n}\right)^y$, and V_n, P_n are the nominal voltage and power values respectively (typically the MPP values of the PV generator at STC). Then, the normalized coefficients *a*, *b* and *c* are related to the actual values by:

$$A = \frac{P_n}{V_n^2} a \qquad B = \frac{P_n}{V_n} b \qquad C = P_n c \tag{7}$$

The best way to solve the system of equations (6) is using the Gaussian elimination method [13], which guarantees robust and accurate solution. Therefore, the proposed analytical expressions for *a*, *b* and *c* are:

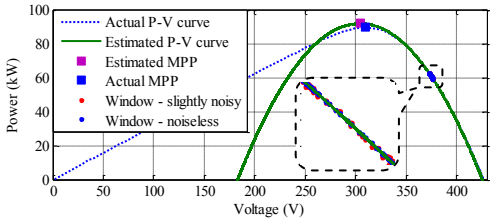

Figure 3: Indicative application scenario of the Quadratic Curve Fitting Estimator maintaining 30% power reserves. The measurement window is depicted for the noiseless and noisy cases.

$$c = \frac{\frac{s_{20}s_{21}}{s_{40}} - s_{01} - \frac{\left(\frac{s_{20}s_{30}}{s_{40}} - s_{10}\right)\left(\frac{s_{21}s_{30}}{s_{40}} - s_{11}\right)}{\frac{s_{30}^2}{s_{40}} - s_{20}}}{\frac{s_{20}^2}{s_{40}} - s_{00} - \frac{\left(\frac{s_{20}s_{30}}{s_{40}} - s_{10}\right)^2}{\frac{s_{30}^2}{s_{40}} - s_{20}}}$$

$$b = \frac{\frac{s_{30}\left(s_{21} - s_{20}c\right)}{s_{40}} + s_{10}c - s_{11}}{\frac{s_{30}^2}{s_{40}} - s_{20}} \qquad (8)$$

$$a = \frac{s_{21} - s_{30}b - s_{20}c}{s_{40}}$$

It is essential to note that a recursive computational procedure is used for the calculation of each sum s_{xy}, rather than a simple summation of the k last terms. In particular, at each step the value of the sum is updated with the latest measurement, while the oldest measurement is removed from the window, thus presenting minimum computational cost:

$$s_{xy}^{k+1} = \sum_{i=2}^{k+1}\left(\frac{V_i}{V_n}\right)^x\left(\frac{P_i}{P_n}\right)^y = \sum_{i=1}^{k}\left(\frac{V_i}{V_n}\right)^x\left(\frac{P_i}{P_n}\right)^y + \left(\frac{V_{k+1}}{V_n}\right)^x\left(\frac{P_{k+1}}{P_n}\right)^y - \left(\frac{V_1}{V_n}\right)^x\left(\frac{P_1}{P_n}\right)^y \qquad (9)$$

$$= s_{xy}^{k} + \left(\frac{V_{k+1}}{V_n}\right)^x\left(\frac{P_{k+1}}{P_n}\right)^y - \left(\frac{V_1}{V_n}\right)^x\left(\frac{P_1}{P_n}\right)^y$$

4 SIMULATIONS

In order to evaluate the proposed control strategy and estimation method efficiency, a 100 kW PV plant is modeled in MATLAB/Simulink according to the block diagram of Figure 1. The system response is simulated in simultaneous changes of the irradiance and reserve command, both in a noiseless (Figure 4) and a slightly noisy environment (Figure 5). Three different window lengths (number of past measurements) are considered, while values of the other parameters adopted are given in Table I.

In Figure 4, the simulation results are depicted for the noiseless scenario. The irradiance profile is trapezoidal at a high rate of 40 W/m^2 per second, which is considered a rapidly changing irradiance [14], while simultaneous step changes from 0% to 40% are assumed for the reserves command (Figure 4(a)).

Table I: Parameters of the simulated system

Parameter	Value
Sampling frequency	25kHz
Control frequency	100Hz
LPF time constant	200ms
Window length	100, 1750, 10000 samples
Noise power	80, ∞ SNR

In Figure 4(b), the values of the normalized coefficients a (continuous lines), b (dashed lines), and c (dotted lines) are depicted for the three window lengths in different color. Ignoring the initialization transients of the first second, the results for the three window lengths almost coincide at the time intervals 1-3 s and 8-10 s where the irradiance remains constant. This means that the window length does not matter in constant operating conditions where the *P-V* curve does not change. On the other hand, when the irradiance increases (3-8 s) or decreases (10-13 s) the 10,000 samples case proves to be unstable, presenting fluctuations of the estimated coefficients. This happens because when the window length is too large, the measurements correspond to several different *P-V* curves due to irradiance variation, rather than a single characteristic.

On the contrary, step changes on the reserves command do not affect the dynamic response of the estimation. They only affect the absolute values, which converge to slightly different levels depending on how much the operating point deviates from the MPP. This is because the appropriateness of the quadratic equation to model the actual *P-V* curve decreases when operating far from the MPP. The accuracy in estimating the maximum available power P_{max} is shown in Figure 4(c). As far as the 100 (green color) and 1,750 (red color) window lengths are concerned, the estimation proves to be sufficiently accurate during the entire simulation period, while the greater errors are presented at the 4-9 s time interval when the reserves command is the highest. The 10,000 samples case (orange color) presents undesired fluctuations of the P_{max} estimate as discussed above.

The output power of the PV generator using either of the window lengths is compared to the requested power in Figure 4(d). As expected, the small and medium window lengths provide best results. Similar observations are made for the reference voltage V_{ref} and duty cycle D in Figure 4(e)-(f) respectively, where waveforms for the 100 and 1,750 samples cases are smooth and stable, whereas undesired fluctuations appear with the 10,000 window length.

Figure 5 is of particular interest, illustrating results of the same simulation as Figure 4, except for the inclusion of noise in measurements. In Figure 5(b), it is shown that the estimated coefficients using the 100 samples window present high frequency fluctuations. This is due to noise, which introduces stochasticity and lowers the dependability of the measured samples. However, given the zero mean value of noise (AWGN), the bigger the set of measurements is, the better curve fitting is achieved. The 1,750 window length case presents quite stable estimations, almost identical to the noiseless scenario, effectively suppressing noise. Nevertheless, the window length should not be chosen too large, since this could hamper the adaptation of the algorithm at rapidly changing irradiance conditions. This is the case of the 10,000 samples, which proves to be unstable when the

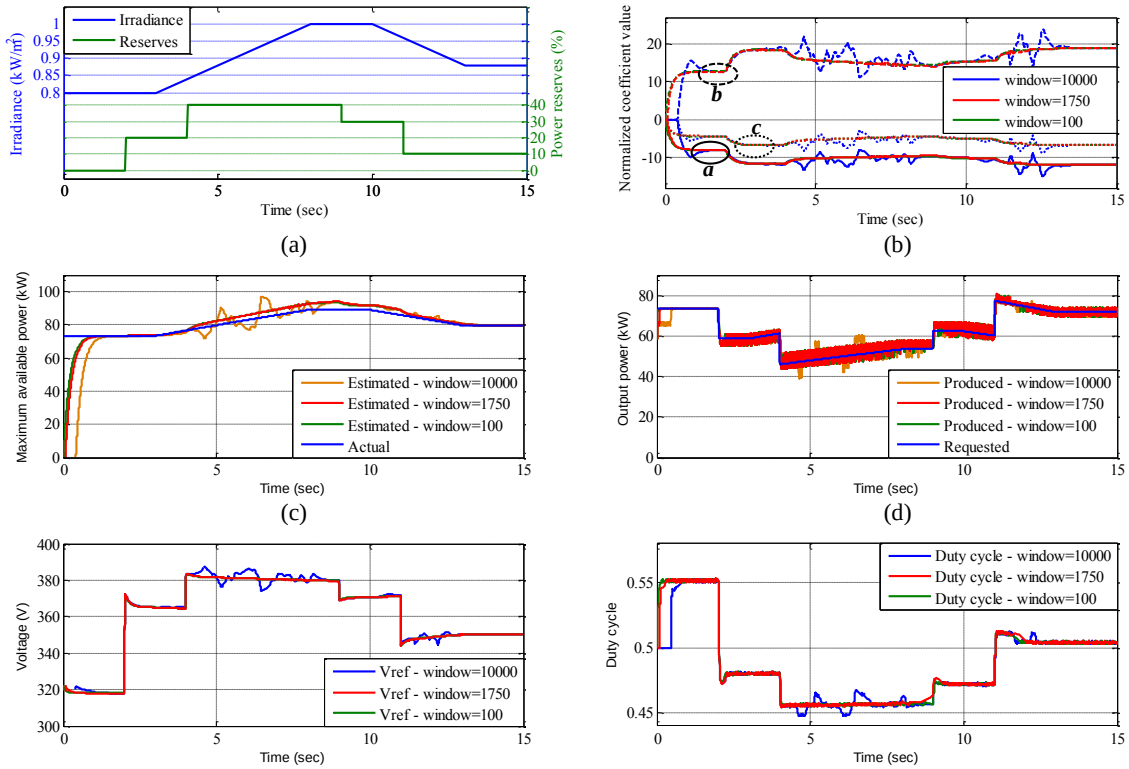

Figure 4: Indicative scenario of system response with various windows lengths to simultaneous irradiance and reserve command changes in a **noiseless** environment. (a) Trapezoidal irradiance variation and step reserve commands, (b) estimated values of the normalized coefficients *a*, *b* and *c*, (c) actual and estimated available maximum power P_{max}, (d) requested and actual output power, (e) operating and reference voltage V_{ref}, and (f) duty cycle *D*.

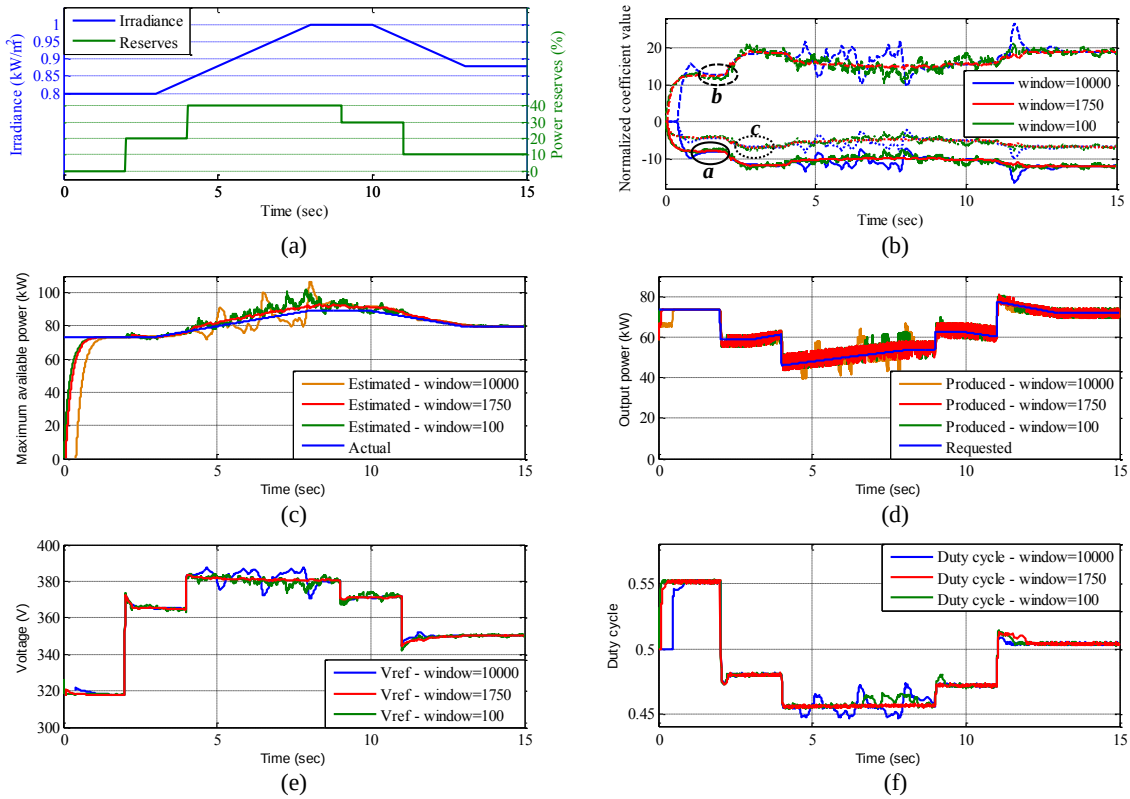

Figure 5: Indicative scenario of system response with various windows lengths to simultaneous irradiance and reserve command changes in a **noisy** environment. (a) Trapezoidal irradiance variation and step reserve commands, (b) estimated values of the normalized coefficients *a*, *b* and *c*, (c) actual and estimated available maximum power P_{max}, (d) requested and actual output power, (e) operating and reference voltage V_{ref}, and (f) duty cycle *D*.

irradiance changes as in the noiseless scenario.

These observations are verified in Figure 5(c)-(f), as well. Results using a measurement window of 100 samples are no longer acceptable, unlike the noiseless scenario of Figure 4, whereas the 1,750 window length presents excellent results at simultaneous irradiance and reserve command changes, including noise. Consequently, the length of the measurements window should be chosen large enough to limit the effect of noise, without compromising the tracking performance of the P_{max} estimator during irradiance variations.

5 CONCLUSION

In this paper, an enhanced control strategy for a PV system to maintain active power reserves is introduced. A quadratic curve fitting algorithm is employed to estimate the *P-V* curve, and thus permit operation at a suboptimal output setpoint issued by the grid operator. The equations involved are explicit, without iterative procedures, leading to a simple and computationally efficient implementation, suitable for the firmware of the microcontroller of the DC/DC converter. The estimation method introduced has an inherent robustness against noise, due to the curve fitting on several samples involved, in contrast to other approaches found in literature which utilize only a few past measurements.

Detailed simulations are performed in MATLAB/Simulink for a PV system during rapid irradiance variations and reserve command changes, assuming both a noiseless and a noisy environment. Time domain simulations demonstrate that the most critical factor affecting the system response is the window length used for the curve fitting procedure, as a tradeoff exists between immunity to noise and tracking performance during irradiance changes. For this purpose, a detailed discussion is provided regarding the optimum length of the latter, which is determined by the noise power and the rate of irradiance variation.

6 ACKNOWLEDGMENTS

Mr. E. Batzelis and Mr. Nanou are supported in their PhD studies by "IKY Fellowships of Excellence for Postgraduate Studies in Greece - Siemens Program".

7 REFERENCES

[1] M. Datta, T. Senjyu, A. Yona, T. Funabashi, and C. H. Kim, "A Frequency-Control Approach by Photovoltaic Generator in a PV–Diesel Hybrid Power System," *IEEE Trans. Energy Convers.*, vol. 26, no. 2, pp. 559-571, Jun. 2011.

[2] G. Delille, B. François, and G. Malarange, "Dynamic Frequency Control Support by Energy Storage to Reduce the Impact of Wind and Solar Generation on Isolated Power System's Inertia," *IEEE Trans. Sustain. Energy*, vol. 3, no. 4, pp. 931-939, Oct. 2012.

[3] A. Hoke, and D. Maksimovic, "Active Power Control of Photovoltaic Power Systems," in *Proc. 2013 1st IEEE Conf. Technologies for Sustainability (SusTech)*, Portland, OR, Aug. 1-2, 2013, pp. 70-77.

[4] V. A. K. Pappu, B. H. Chowdhury, and R. Bhatt, "Implementing Frequency Regulation Capability in a Solar Photovoltaic Power Plant," in *Proc. 2010 North American Power Symposium (NAPS)*, Arlington, TX, Sept. 26-28, 2010, pp. 1-6.

[5] A. F. Okou, O. Akhri, R. Beguenane, and M. Tarbouchi, "Nonlinear Control Strategy Insuring Contribution of PV Generator to Voltage and Frequency Regulation," in *Proc. 2012 6th IET Int. Conf. Power Electronics, Machines and Drives (PEMD)*, Bristol, Mar. 27-29, 2012, pp. 1-5.

[6] R. G. Wandhare, and V. Agarwal, "Novel Control Scheme for High Power Centralized PV-Grid System to Realize Functionalities of AVR and Governor as in Conventional Generators," in *Proc. 2011 37th IEEE Photovoltaic Specialists Conf. (PVSC)*, Seattle, WA, Jun. 19-24, 2011, pp.002460-002465.

[7] H. Xin, Y. Liu, Z. Wang, D. Gan, and T. Yang, "A New Frequency Regulation Strategy for Photovoltaic Systems Without Energy Storage," *IEEE Trans. Sustain. Energy*, vol. 4, no. 4, pp. 985-993, Oct. 2013.

[8] S. Nanou, A. Papakonstantinou, and S. Papathanassiou, "Control of a PV Generator to Maintain Active Power Reserves during Operation," in *Proc.2012 27th European Photovoltaic Solar Energy Conf. and Exh. (EU PVSEC)*, Frankfurt, Sep. 24-28, 2012, pp. 4059-4063.

[9] S. Nanou, S. Papathanassiou, G. Vokas, "Small Signal Analysis and Gain Scheduling Control of a Photovoltaic DC/DC Converter", in *Proc.2012 27th European Photovoltaic Solar Energy Conf. and Exh. (EU PVSEC)*, Frankfurt, Sep. 24-28, 2012, pp. 3579-3583.

[10] F. S. Pai, R. M. Chao, S. H. Ko, and T. S. Lee, "Performance evaluation of parabolic prediction to maximum power point tracking for PV array," *IEEE Trans. Sustain. Energy*, vol. 2, no. 1, pp. 60-68, Jan. 2011.

[11] W. Xiao, M. G. J. Lind, W. G. Dunford, and A. Capel, "Real-time identification of optimal operating points in photovoltaic power systems," *IEEE Trans.Ind. Electron.*, vol. 53, no. 4, pp. 1017-1026, Jun. 2006.

[12] http://en.wikipedia.org/wiki/Least_squares.

[13] http://en.wikipedia.org/wiki/Gaussian_elimination.

[14] S. Nanou, E. Batzelis, and S. Papathanassiou, "Enhanced MPPT control of a two-stage grid-connected PV system under fast-changing irradiance conditions," in *Proc. 28th European Photovoltaic Solar Energy Conf. and Exh. (EU PVSEC)*, Paris, Sep. 24-28, 2013, pp. 3399-3403.